Quantum Electronics **50** (9) 855–860 (2020) ©2020 Kvantovaya Elektronika and IOP Publishing Limited

NANOPARTICLES https://doi.org/10.1070/QEL17318

Synthesis of TiO_2 nanoparticles decorated with gold nanoclusters using pulsed laser ablation in liquid

S.O. Gurbatov, N. Mintcheva, S. Iwamori, S.A. Kulinich, A.A. Kuchmizhak

Abstract. **Amorphous spherical titanium dioxide (TiO_2) nanoparticles, decorated gold nanoparticles, are shown to be formed under irradiation of commercial TiO_2 nanopowders dispersed in aqueous solution of hydrogen tetrachloroaurate ($HAuCl_4$) by second-harmonic nanosecond pulses of an Nd:YAG laser. It is found that these hybrid nanostructures are formed during laser-induced remelting of the initial nanoparticles, stimulated by gold nanoclusters (providing more efficient absorption of visible laser radiation by titanium dioxide) recovered on their surface. The morphology and chemical composition of the newly formed hybrid nanomaterials are investigated in detail by electron microscopy, Raman spectroscopy, and energy-dispersive analysis. It is shown that the average size and number of gold nanoparticles recovered on the TiO_2 surface can be controlled by varying the concentration ratio of the initial nanomaterial and $HAuCl_4$. A spectroscopic analysis of light scattering by single hybrid nanoparticles and the results of numerical calculation of the structure of electromagnetic fields near their surface indicate good prospects of these hybrid nanomaterials for various applications in modern optics, optoelectronics, and nanophotonics; for example, for designing chemo- and biosensor platforms and new-generation solar cells.**

Keywords: *hybrid nanomaterials, laser ablation in liquid, titanium dioxide.*

1. Introduction

The study of the optical properties of nanoparticles based on metals supporting light-induced resonance oscillations of electron density (localised plasmon resonance) and submicron structures based on insulators and semiconductors with a high refractive index has been one of the main lines of fundamental and applied research for several decades in such actively developing fields as nanophotonics, plasmonics, optoelectronics, etc. [1–4]. The unflagging popularity of the aforementioned nanomaterials is related to their unique optical properties. In particular, multiply amplified electromagnetic fields ('hot points') localised on the subwavelength scales can be generated near the surface of plasmon-active nanoparticles, whereas submicron dielectric cavities maintain optically induced electric and magnetic responses (Mie resonances), providing significant field amplification in the particle and a possibility of controlling the directional radiation pattern [5, 6]. Obviously, the combination of unique optical properties of dielectric and plasmonic materials within a unified miniature system will make it possible to combine a controlled and tunable magnetic optical response with a high degree of electromagnetic field localisation and amplification, thus opening ways to form nanomaterials with unique optical properties, optimised ratio of radiative and nonradiative losses, and extended working spectral range [7, 8]. In particular, hybrid nanostructures of this type are promising for implementing nanoscale light control devices and optical switches; enhancing nonlinear optical effects; and designing chemo- and biosensors based on effects of surface-enhanced photoluminescence, Raman scattering, and IR absorption [9–12]. Note also that hybrid metal–dielectric nanomaterials are being actively investigated in various photo- and electrocatalytic applications [13, 14].

At the same time, the difference in the characteristic sizes of semiconductor and dielectric nanoparticles (200–500 nm in diameter) and plasmonic nanoparticles with sizes less than 50 nm, which are necessary to generate a resonance response in the visible spectral range from both functional parts makes the preparation of hybrid metal–insulator nanostructures a fairly time-consuming task, even with the aid of advanced and highly expensive lithography methods. Using liquid-phase chemistry technologies, one can obtain nanoparticles of different metals on the functionilised surface of dielectric particles [15, 16]. However, this approach barely makes it possible to control the size of metal nanoparticles, which is the main factor determining their optical properties. In addition, the use of different toxic materials during chemical synthesis of hybrid nanomaterials does not meet the environmental safety requirements, which become more and more stringent.

In recent years, pulsed laser ablation in liquid (PLAL) appeared to be a universal, highly efficient, and economically justified technology for synthesising nanomaterials and various functional nanostructures [17–21]. In contrast to the methods of liquid-phase chemical synthesis, PLAL is carried out under conventional environmental conditions and does not require extreme temperatures and/or pressures. In addition, it is chemically simple and ecologically pure technology,

S.O. Gurbatov, A.A. Kuchmizhak Institute of Automation and Control Processes, Far Eastern Branch, Russian Academy of Sciences, ul. Radio 5, 690041 Vladivostok, Russia; Far Eastern State University, ul. Sukhanova 8, 690091 Vladivostok, Russia;
e-mail: gurbatov_slava@mail.ru;
N. Mintcheva Department of Chemistry, University of Mining and Geology, Sofia 1700, Bulgaria; Research Institute of Science and Technology, Tokai University, Hiratsuka, Kanagawa 259-1292, Japan;
S. Iwamori Research Institute of Science and Technology, Tokai University, Hiratsuka, Kanagawa 259-1292, Japan;
S.A. Kulinich Far Eastern State University, ul. Sukhanova 8, Vladivostok, 690091 Russia; Research Institute of Science and Technology, Tokai University, Hiratsuka, Kanagawa 259-1292, Japan

Received 2 March 2020; revision received 10 April 2020
Kvantovaya Elektronika **50** (9) 855–860 (2020)
Translated by Yu.P. Sin'kov

which does not imply occurrence of many minor products and use of catalysts. These factors provide formation of chemically pure nanomaterials with a high surface activity. Intense laser irradiation forms unique physical conditions for generating nanomaterials: colossal pressures and temperatures (up to several thousand kelvin), due to which nanoparticles with unique metastable phases can be obtained [22–30]. In addition, this method even makes it possible to synthesise nanostructures with complex chemical composition and morphology (for example, nanoparticles of core–shell type, alloyed and decorated nanoparticles, hollow and nonspherical ones, etc.). Their main characteristics can be controlled by varying the main laser-irradiation parameters, as well as the liquid and target types. At the same time, only several studies on the use of PLAL for fabricating decorated plasmonic nanoparticles of dielectric nanomaterials have been published to date; moreover, the potential of these hybrid nanomaterials for solving nanophotonics problems has barely been discussed [31–33].

In this paper we demonstrate a possibility of forming spherical titanium dioxide (TiO_2) nanoparticles decorated with gold nanoparticles under irradiation of commercial TiO_2 nanopowders dispersed in an aqueous hydrogen tetrachloroaurate ($HAuCl_4$) solution by second-harmonic nanosecond Nd:YAG laser pulses. It is established that the formation of these hybrid nanostructures occurs during laser-induced remelting of initial nanoparticles, stimulated by gold nanoclusters reconstructed on their surfaces, which provide more efficient absorption of visible laser light by titanium dioxide. A possibility of controlling the average size and density of gold nanoparticles decorating the TiO_2 surface by varying the concentration ratio of the initial nanoparticles and $HAuCl_4$ is demonstrated. A spectroscopic analysis of the specific features of light scattering by single hybrid nanoparticles and the corresponding numerical calculations of the structure of electromagnetic fields near their surface indicate good prospects of these hybrid nanomaterials in different applications of modern optics, optoelectronics, and nanophotonics, for example, in designing chemo- and biosensor systems and new-generation solar cells.

2. Materials and methods

The initial material for fabricating spherical TiO_2 nanoparticles decorated with gold was commercially available TiO_2 nanopowder (anatase crystalline phase, Wako Chemicals, 99.99%) with an average particle size of 120 nm. First TiO_2 nanoparticles were dispersed in deionised water (mass fraction of 0.001% in suspension) under the action of ultrasonic homogeniser; then the suspension (7.5 mL in volume) was transferred to a quartz cell with a volume of $3 \times 3 \times 6$ cm, and an $HAuCl_4$ aqueous solution with a concentration of 10^{-3} M was added to it (in amounts of 0.25, 0.5, and 0.75 mL for different cases). After this procedure, the suspension was irradiated for 2 h by a focused nanosecond pulsed laser beam (Quantel Ultra 50 laser, wavelength 532 nm, pulse width 8 ns, maximum pulse repetition rate 20 Hz) (Fig. 1a). The laser energy was 25 mJ pulse^{-1}; it was monitored by a Coherent FieldMaxII-TOP power meter. The laser beam was focused to the cell center by a lens with a focal length of 10 cm. During the irradiation the suspension was continuously stirred by a magnetic agitator with a speed of 600 vol min^{-1}. All experiments on laser irradiation were performed under standard environmental conditions at room temperature. The products obtained after the irradiation were separated using centrifugation, washed with deionised water, and passed through a membrane filter to remove $HAuCl_4$ residues.

The nanomaterial morphology was monitored in all processing stages by high-resolution electron microscopy (Carl Zeiss, Ultra 55+). To this end, a drop of dispersed product (2.5 mL in volume) was deposited on a crystalline silicon wafer and dried at 70 °C. Energy-dispersive X-ray spectroscopy (EDXS) was applied to determine the chemical composition of hybrid nanoparticles. The phase composition of single nanoparticles was investigated by Raman spectroscopy. The Raman spectra of nanoparticles deposited on a silver mirror were measured upon excitation by stable semiconductor laser sources (central wavelengths 532 and 780 nm, average power 50 W), whose radiation was focused on the sample surface by an objective with NA = 0.95. The scattered radiation was collected by the same objective and analysed using a grating spectrometer equipped with a cooled CCD camera (Andor Shamrock 303i or Andor Newton 935).

Similar optical system and spectrometer were used to analyse the dark-field scattering spectra of single hybrid nanoparticles. In these experiments the surface of a glass slide substrate with deposited hybrid nanoparticles was illuminated by broadband light beam from a supercontinuum generator, incident at an angle of 20° with respect to the normal to the sample surface, which excluded the possibility for light directly reflected from the sample to arrive at the microscope objective. The structures and intensities of electromagnetic fields localised near hybrid $Au–TiO_2$ nanoparticles were calculated by numerical solution of the Maxwell equations using the finite-difference time-domain method, implemented in the commercial software Lumerical Solutions.

3. Results and discussion

An analysis of the SEM images of initial TiO_2 nanopowder deposited on a silicon substrate showed that, prior to pulsed laser irradiation, the nanoparticles had an irregular shape and an average size of ~120 nm (Fig. 1b). Primarily, we should note that the initial nanoparticles can barely absorb the 532-nm laser radiation, which was used in this work. This is evidenced, in particular, by the fact that pulsed laser irradiation did not lead to any significant modification of the shape and size of initial nanoparticles in the absence of $HAuCl_4$ in their suspension. At the same time, according to the spectrophotometry data (which are not discussed here), addition of $HAuCl_4$ does not change on the whole the absorption characteristics of the suspension at the aforementioned wavelength. In our opinion, the aforementioned features are indicative of the key role of gold nanoclusters reconstructed on the titanium dioxide surface during laser-induced melting/modification of optically transparent TiO_2 nanoparticles. This conclusion is partially confirmed by the fact that the reduction of gold on the surfaces of initial particles may occur without laser irradiation, for example, under the action of day light, ultrasound, vibrations, etc.

It is beyond the scope of this study to establish which of the aforementioned mechanisms plays the key role. However, for demonstration purposes, we analysed the morphology of initial nanopowders exposed for 2 h in a solution of deionised water and 0.25 mL $HAuCl_4$ aqueous solution with a concentration of 10^{-3} M, stirred by a magnetic agitator; the thus prepared suspension is identical to those used in the experiments on laser ablation in liquid. An analysis of the SEM images

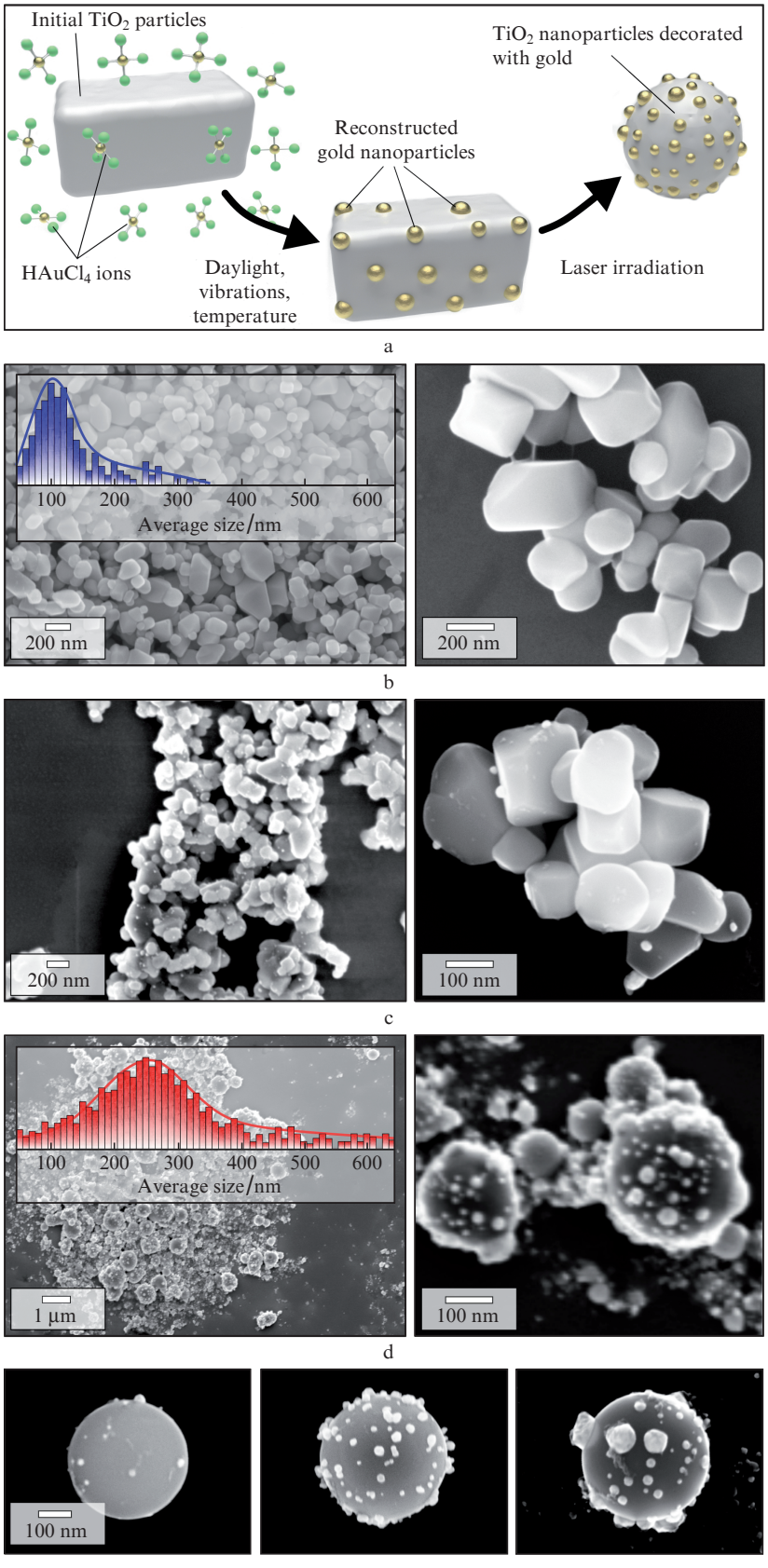

Figure 1. (a) Schematic of the main stages of the formation of spherical nanoparticles and (b–e) SEM images of (b) initial TiO_2 nanoparticles, (c) similar nanoparticles exposed for 2 h in a mixed aqueous solution of $HAuCl_4$, (d) nanoparticles produced as a result of irradiation of a suspension of initial TiO_2 nanoparticles in an $HAuCl_4$ aqueous solution, and (e) TiO_2 particles decorated with gold and formed at different initial contents of $HAuCl_4$ in the solution. The SEM images in the right column (b–d) are given on an enlarged scale; the characteristic size distributions of TiO_2 nanoparticles before and after their irradiation in an $HAuCl_4$ aqueous solution are shown in the insets in panels b and d.

clearly shows the formation of gold nanoclusters ~15 nm in size on the surface of initial TiO_2 nanoparticles (Fig. 1c). A 2-h irradiation of the aforementioned nanoparticle suspensions by intense laser pulses leads to remelting (induced by deposited gold clusters) of the initial nanomaterial of irregular shape into nanospheres with an average diameter of about 250 nm (Fig. 1d). Varying the $HAuCl_4$ concentration in the solution, one can control the degree of decoration (the number and average size of deposited gold nanoparticles) of the hybrid nanomaterials (Fig. 1e). It is noteworthy that all particles of the initial nanopowder are transformed into spherical nanoparticles under this impact, while the increase in the average size of newly formed nanoparticles indicates that nanospheres can be formed as a result of alloying two or more nanoparticles.

An analysis of the results of a series of similar experiments, performed for different times of laser irradiation of suspensions, showed that, for a fixed initial amount of $HAuCl_4$, a longer term irradiation (above 2 h) does not increase the degree of decoration of TiO_2 particles but leads to an increase in their average size and formation of microspheres with a diameter up to 1.5 μm, which is apparently due to the secondary remelting of titanium dioxide particles. At the same time, at a shorter irradiation time, the SEM images of nanomaterials revealed the presence of unmodified nanoparticles of the initial material.

A comparative analysis of the energy-dispersive X-ray spectra of the initial and laser-irradiated nanomaterials demonstrates their only difference: the presence of characteristic gold peaks in the spectra of irradiated $Au-TiO_2$ particles (Fig. 2a). At the same time, a comparison of the Raman spectra of hybrid nanoparticles with those of the initial nanomaterial indicates that their crystal structures significantly differ. In particular, all characteristic anatase peaks (denoted by circles in Fig. 2b), which are present in the Raman spectra of the initial nanomaterial, are absent in the Raman spectrum of $Au-TiO_2$ nanoparticles. The Raman spectra of these hybrid nanoparticles, independent of the degree of decoration with gold particles, are wide bands, in which only two weak peaks can be identified above the noise level (denoted by triangles in Fig. 2b), which are presumably due to the inclusions of rutile crystalline phase of titanium dioxide [34]. These inclusions may be located in the nanoparticle bulk, whereas the external shell may be a disordered (amorphous) Ti_2O_3 layer [34, 35]. This suggestion is partially confirmed by the fact that the Raman signal from surface layers is expected to be enhanced by gold nanoparticles. The Raman spectra of hybrid nanoparticles, measured using sources with wavelengths of 532 and 780 nm, did not show any significant distinctions. We are planning to continue the detailed study of the crystal structure of PLAL-produced decorated $Au-TiO_2$ nanoparticles.

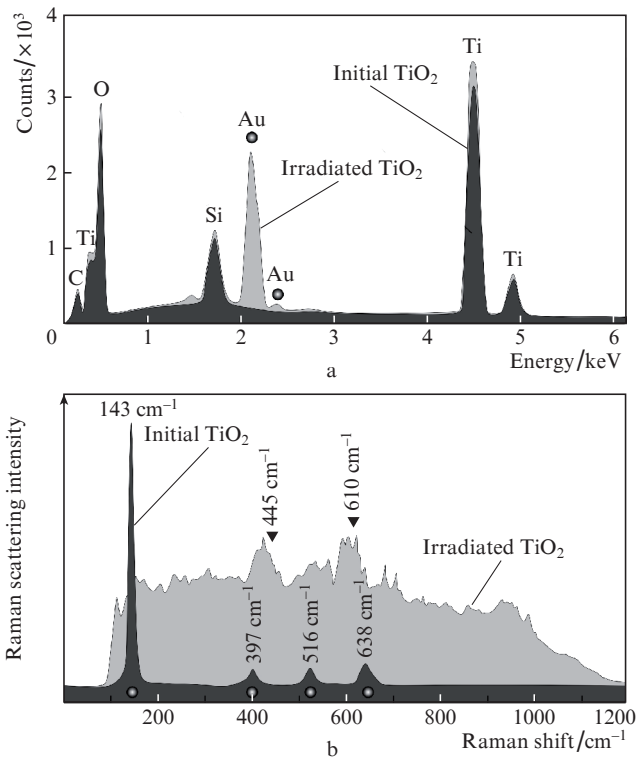

Figure 2. (a) EDXS spectra of initial and laser-pulse irradiated TiO_2 nanoparticles with indication of the main identified chemical elements and (b) averaged Raman spectra of initial and irradiated TiO_2 nanoparticles, with identified positions of main Raman lines of anatase (circles) and rutile (triangles).

Spherical dielectric nanoparticles having a high refractive index ($n > 2$) are known to maintain electric and magnetic Mie resonances [36]. Decoration of these subwavelength resonance structures with plasmon-active nanoparticles of noble metals, whose localised plasmon resonances coincide in frequency with Mie resonances, opens prospects for various applications in sensorics, nanoscale light control, and enhancement of nonlinear effects [7, 8, 37]. To demonstrate the potential of PLAL-produced hybrid nanoparticles for the aforementioned applications, we measured and analysed dark-field light scattering spectra of single hybrid $Au-TiO_2$ nanoparticles with different degrees of decoration in the visible spectral range. To carry out these measurements, hybrid nanoparticles were precipitated on a glass substrate surface from a drop; the nanoparticle concentration was chosen so as to provide precipitation and subsequent analysis of individual nano-objects.

Figure 3a shows two representative dark-field scattering spectra of single hybrid nanoparticles having the same diameter (~610 nm) but significantly different degrees of decoration. The spectra of both particles demonstrate a number of features in the visible region; they coincide in position and, apparently, are due to high-order Mie resonances, which are maintained by the dielectric base of hybrid nanoparticle (the position of the main magnetic dipole Mie resonance for a particle with a diameter D and refractive index n is determined by the product Dn). At the same time, the intensity of dark-field scattering signal in the red spectral region (550–750 nm) for a strongly decorated particle increases twice. This is due to the contribution (expected in this range) of plasmon-induced resonance scattering of single gold nanoparticles located on the TiO_2 surface to the total scattering signal. The red shift of the scattering band of plasmon-active clusters can be explained by their hemispherical shape; the latter provides good contact with the TiO_2 surface, which has a high refractive index [38]. In addition, the interacting electromagnetic fields of nanoparticles spaced by a distance smaller than 30 nm may also contribute to scattering in this wavelength range. In the case of magnetic Mie resonances the electromagnetic field is mainly concentrated within a particle; however, the presence of plasmonic nanoclusters on its surface makes it possible to convert a part of radiation 'localised' in the particle for more efficient pumping of fields in the vicinity of plasmonic nanoparticles. This is clearly illustrated by comparative numerical calcula-

tions of the structure and intensity of electromagnetic fields near conventional (TiO_2) and hybrid ($Au-TiO_2$) nanoparticles 610 nm in diameter (Figs 3b, 3c). Obviously, the presence of gold nanoparticles decreases the Q factor of Mie resonances, which also manifests itself in the measured scattering spectra of two hybrid nanoparticles beyond the plasmonic scattering band. However, the electromagnetic field amplitude is significantly increased near the surface of decorating nanoparticles at the wavelengths coinciding with Mie resonance wavelengths, which is important for some practical applications.

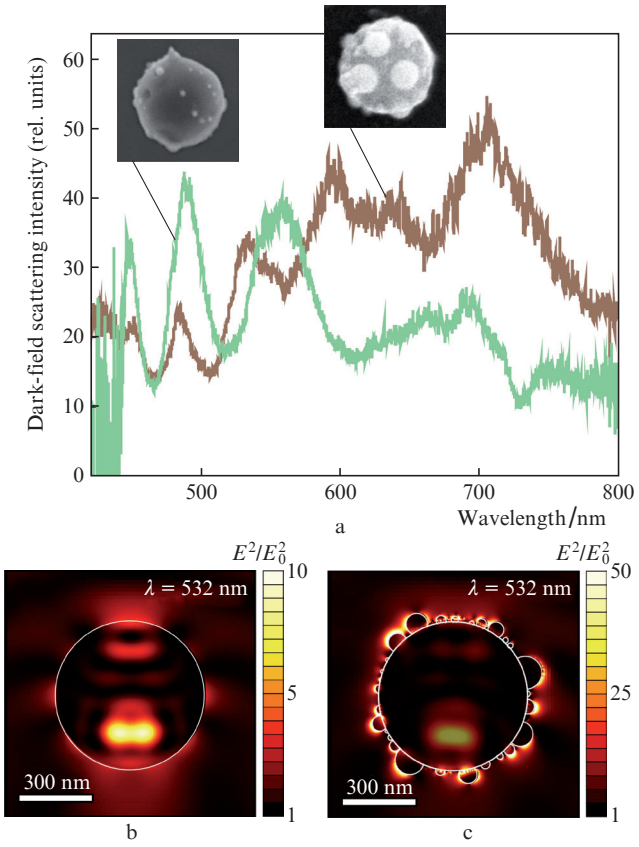

Figure 3. (a) Dark-field light scattering spectra of single TiO_2 nanoparticles with identical diameter (610 nm) but different degrees of decoration with gold nanoparticles. The insets show SEM images of the corresponding nanoparticles. (b, c) Calculated (for an excitation x-polarised source wavelength of 532 nm) distributions of normalised electromagnetic field intensity E^2/E_0^2 near the surface and in the bulk of these nanoparticles.

4. Conclusions

Using a simple and high-efficiency PLAL method, we demonstrated a possibility of fabricating new promising hybrid nanomaterials: amorphous spherical TiO_2 nanoparticles (with an average diameter of 250 nm) decorated with gold nanoclusters. It was experimentally shown that, changing the concentration ratio of the initial TiO_2 nanoparticles and $HAuCl_4$ in suspension, one can control the average size and number of deposited gold nanoparticles. At the same time, the average size of initial TiO_2 nanoparticles is expected to determine the diameter of the PLAL-produced spherical TiO_2 nanoparticles decorated with gold nanoclusters. The possibility of controlling the main geometric parameters of hybrid nanoparticles opens ways to use them in various applications of modern photonics, including the design of chemo- and biosensors and new-generation solar cells; we are planning to investigate this issue in detail.

Acknowledgements. S.O. Gurbatov acknowledges the support of the Russian Science Foundation (Project No. 19-79-00214). A.A. Kuchmizhak acknowledges the Foundation of the President of the Russian Federation for Support of Young Russian Scientists–Candidates of Sciences (Grant No. MK-3258.2019.8).

References

1. Maier S.A. *Plasmonics: Fundamentals and Applications* (Berlin: Springer Science & Business Media, 2007).
2. Fang Z., Peng Q., Song W., Hao F., Wang J., Nordlander P., Zhu X. *Nano Lett.*, **11**, 893 (2011).
3. Arbabi A., Horie Y., Bagheri M., Faraon A. *Nature Nanotech.*, **10**, 937 (2015).
4. Kuchmizhak A., Gurbatov S., Kulchin Yu., Vitrik O. *Opt. Commun.*, **356**, 1 (2015).
5. Pavlov D., Syubaev S., Kuchmizhak A., Gurbatov S., Vitrik O., Modin E., Kudryashov S., Wang X., Juodkazis S., Lapine M. *App. Surf. Sci.*, **469**, 514 (2019).
6. Fu Y.H., Kuznetsov A.I., Miroshnichenko A.E., Yu Y.F., Luk'yanchuk B. *Nat. Commun.*, **4**, 1527 (2013).
7. Zuev D.A., Makarov S.V., Mukhin I.S., Milichko V.A., Starikov S.V., Morozov I.A., Shishkin I.I., Krasnok A.E., Belov P.A. *Adv. Mater.*, **28**, 3087 (2016).
8. Jiang R., Li B., Fang C., Wang J. *Adv. Mater.*, **26**, 5274 (2014).
9. Liu W., Miroshnichenko A.E., Neshev D.N., Kivshar Y.S. *ACS Nano*, **6**, 5489 (2012).
10. Wang H., Liu P., Ke Y., Su Y., Zhang L., Xu N., Deng S., Chen H. *ACS Nano*, **9**, 436 (2015).
11. Devilez A., Stout B., Bonod N. *ACS Nano*, **4**, 3390 (2010).
12. Rusak E., Staude I., Decker M., Sautter J., Miroshnichenko A.E., Powell D.A., Neshev D.N., Kivshar Y.S. *Appl. Phys. Lett.*, **105**, 221109 (2014).
13. Damato T.C., de Oliveira C.C., Ando R.A., Camargo P.H. *Langmuir*, **29**, 1642 (2013).
14. Kochuveedu S.T., Kim D.P., Kim D.H. *J. Phys. Chem. C*, **116**, 2500 (2012).
15. Wang Y., Fang H.B., Zheng Y.Z., Ye R., Tao X., Chen J.F. *Nanoscale*, **7**, 19118 (2015).
16. Ghosh Chaudhuri R., Paria S. *Chem. Rev.*, **112**, 2373 (2012).
17. Zhang D., Gökce B., Barcikowski S. *Chem. Rev.*, **117**, 3990 (2017).
18. Reich S., Schönfeld P., Wagener P., Letzel A., Ibrahimkutty S., Gökce B., Barcikowski S., Menzel A., dos Santos Rolo T., Plech A. *J. Colloid Interface Sci.*, **489**, 106 (2017).
19. Taccogna F., Dell'Aglio M., Rutigliano M., Valenza G., De Giacomo A. *Plasma Sources Sci. Technol.*, **26**, 045002 (2017).
20. Barmina E.V., Shafeev G.A. *Quantum Electron.*, **48**, 637 (2018) [*Kvantovaya Elektron.*, **48**, 637 (2018)].
21. Serkov A.A., Kuz'min P.G., Rakov L.I., Shafeev G.A. *Quantum Electron.*, **46**, 713 (2016) [*Kvantovaya Elektron.*, **46**, 713 (2016)].
22. Feng Y., Li Z., Liu H., Dong C., Wang J., Kulinich S.A., Du X.W. *Langmuir*, **34**, 13544 (2018).
23. Mintcheva N., Aljulaih A.A., Bito S., Honda M., Kondo T., Iwamori S., Kulinich S.A. *J. Alloy. Compd.*, **747**, 166 (2018).
24. Niu K.Y., Kulinich S.A., Yang J., Zhu A.L., Du X.W. *Chem.–Eur. J.*, **18**, 4234 (2012).
25. Honda M., Goto T., Owashi T., Rozhin A.G., Yamaguchi S., Ito T., Kulinich S.A. *Phys. Chem. Chem. Phys.*, **18**, 23628 (2016).
26. Zeng H.B., Du X.W., Singh S.C., Kulinich S.A., Yang S.K., He J.P., Cai W.P. *Adv. Funct. Mater.*, **22**, 1333 (2012).
27. Goncharova D.A., Kharlamova T.S., Lapin I.N., Svetlichnyi V.A. *J. Phys. Chem. C*, **123**, 21731 (2019).
28. Mintcheva N., Aljulaih A.A., Wunderlich W., Kulinich S.A., Iwamori S. *Materials*, **11**, 1127 (2018).

29. Kondo T., Sato Y., Kinoshita M., Shankar P., Mintcheva N.N., Honda M., Iwamori S., Kulinich S.A. *Jpn. J. Appl. Phys.*, **56**, 080304 (2017).
30. Kulinich S.A., Kondo T., Shimizu Y., Ito T. *J. Appl. Phys.*, **113**, 033509 (2013).
31. Mintcheva N., Srinivasan P., Rayappan J.B.B., Kuchmizhak A.A., Gurbatov S.O., Kulinich S.A. *Appl. Surf. Sci.*, **507**, 145169 (2020).
32. Saraeva I.N., Van Luong N., Kudryashov S.I., Rudenko A.A., Khmelnitskiy R.A., Shakhmin A.L., Kharin A.Y., Ionin A.A., Zayarny D.A., Tung D.H., Duong P.V., Minh P.H. *J. Photochem. Photobiol. A*, **360**, 125 (2018).
33. Liu P., Chen H., Wang H., Yan J., Lin Z., Yang G. *J. Phys. Chem. C*, **119**, 1234 (2015).
34. Tian M., Mahjouri-Samani M., Gyula Eres G., Sachan R., Yoon M., Chisholm M.F., Wang K., Puretzky A.A., Rouleau C.M., Geohegan D.B., Duscher G. *ASC Nano*, **9** (10), 10482 (2015).
35. Zuñiga-Ibarra V.A., Shaji S., Krishnan B., Johny J., Kanakkillam S.S., Avellaneda D.A., Aguilar Martinez J.A., Das Roya T.K., Ramos-Delgado N.A. *Appl. Surf. Sci.*, **483**, 156 (2019).
36. Kuznetsov A.I., Miroshnichenko A.E., Brongersma M.L., Kivshar Y.S., Luk'yanchuk B. *Science*, **354**, 846 (2016).
37. Larin A.O., Nominé A., Ageev E.I., Ghanbaja J., Kolotova L.N., Starikov S.V., Bruyére S., Belmonte T., Makarov S.V., Zuev D.A. *Nanoscale*, **12**, 1013 (2020).
38. Gurbatov S., Vitrik O., Kulchin Y., Kuchmizhak A. *Sci. Rep.*, **8**, 1 (2018).